NASA CONTRACTOR REPORT 172323

# LIQUID CRYSTAL POLYESTER-CARBON FIBER COMPOSITES

Tai-shung Chung

Celanese Research Company
a division of
Celanese Corporation
Summit, New Jersey 07901

Contract No. NAS1-15749
Task Assignment No. 5
FINAL REPORT
May 1984



National Aeronautics and
Space Administration

Langley Research Center
Hampton, Virginia 23665

TABLE OF CONTENTS

LIST OF ILLUSTRATIONS

LIST OF TABLES

## SECTION 1. INTRODUCTION

The interest in thermoplastic/carbon fiber (CF) composites for the aircraft/aerospace industry is rapidly growing. Thermoplastic materials are more ductile and consequently have higher toughness and impact resistance than their thermoset counterparts. Thermoplastics also offer significant process advantages such as unlimited shelf life and formability when heated, which should result in lower fabrication costs. However, since most thermoplastics have much higher melt viscosity than thermosets, the fabrication process and impregnation mechanism for the two systems are quite different. In addition, because most conventional thermoplastic matrices may crystallize in-situ on the carbon fiber surface, the influence of the surface chemistry of carbon fiber needs to be identified.

In recent years, Celanese has developed a new class of polymeric material based on hydroxynaphthoic acid chemistry, consisting of rigid backbone molecules. These polymers exhibit liquid crystalline order in the melt which produces a high degree of molecular orientation and excellent mechanical properties. Unlike lyotropic liquid crystal polymers, thermotropic liquid crystal polymers (LCP) can be easily processed using convention injection molding, extrusion and melt spinning equipment. The melting point of Celanese LCP materials is highly dependent on the monomer composition of the polymer as well as the polymerization conditions. To facilitate ease of processing on conventional equipment, polymers having melting points in a useable range of 290-310°C have been extensively studied and employed in this work.

Articles fabricated from unfilled LCP materials have mechanical properties at least comparable to conventional short fiber-reinforced engineering resins. Solvent resistance as well as dimensional stability are also generally superior to conventional

thermoplastic resins. Due to the unique mechanical properties and excellent chemical resistance, it is anticipated that these LCP materials will offer advantages as a thermoplastic matrix resin. Work related to fabrication techniques and mechanical properties of LCP/carbon fiber composites is documented in this report.

## SECTION 2. LITERATURE SURVEY

Development of thermoplastic/continuous carbon fiber composites began about a decade ago. Hoggatt investigated polysulfone and phenoxy polymers.[1] Hartness and coworkers studied polyphenylene sulfide (PPS), polyphenylene sulfone, and polyether ether ketone (PEEK) matrices.[2-5] McMahon and Maximovich developed and evaluated Nylon 6,6 and polybutylene terephthalate (PBT) matrices.[6] The effects of various surface finishes on composite performance have been discussed. Sheppard and House evaluated polyimide-capped polysulfone, PPS, polyamide-imide, PEEK and PBT.[7] More detailed studies of PEEK matrix composites were also reported in the recent literature.[8-10]

The effect of the surface chemistry of carbon fiber on the structure of thermoplastic polymer has also been studied. Baer, et al,[11] found that polymer could be epitaxially crystallized from solutions and melted on heterogeneous surfaces to yield a layer of oriented crystallites. In-situ crystallization of polyamides was observed by Fisher et al,[12] and Seifert.[13] Epitaxial crystallization of Nylon 6 and Nylon 6,6 monomers on graphite surfaces was reported by Lando and Frayer.[14] Tuinstra and Baer[15] demonstrated that polyethylene (PE) epitaxially crystallized on single crystals of graphite. Kardos[16] induced nucleated crystallization of polycarbonate on carbon fiber surfaces and found an improvement on composite mechanical properties. Hobbs[17-18] examined isotactic polypropylene crystallization on carbon fibers and showed the importance of substrate geometry on the nucleation

of polymer crystallization from the melt. Cogswell[19] found the crystalline size of PEEK on carbon fiber strongly dependent upon the process conditions.

In 1976, a new class of materials with excellent chemical and mechanical strength was developed by researchers at Tennessee Eastman.[20-22] The extraordinary change in the properties of these thermoplastics can be explained through the physical formation of liquid crystals in the melt. Since then, a variety of liquid-crystal-containing polymers have been invented.[23-31] Because of their lower melt viscosity, they flow easier and offer processing advantages over conventional thermoplastics.

## SECTION 3. MATHEMATICAL MODELLING OF FIBER IMPREGNATION PROCESS

To ensure a high quality of the composite, the resin matrix must flow into the voids among the filaments to cover every hill and valley of the fibers. There are two driving forces for impregnation. One is the external force, and the other is surface tension. The former applies pressure on the melt in order to push it into the fiber bundle; the latter pulls the melt into the filaments by the surface forces between the matrix and the fiber.

Assuming that the surface tension force is negligible and the melt is a power-law fluid, the external pressure needed to push polymer flowing through the nip between two filaments, as shown in Figure 1, can be calculated as follows:

$$\Delta p_1 = Q^n \mu_o \left[\frac{2n+1}{2n}\right]^n \int_{-R}^{R} \left(Ho + R - \sqrt{R^2-x^2}\right)^{-(2n+1)} dx \qquad (1)$$

where n is the power-law index (n=1 for a Newtonian fluid), $\mu_o$ is the viscosity if n=1, Q is the flow rate ($cm^3/sec$), Ho is the distance between two filaments, and R is the radius of the filament.

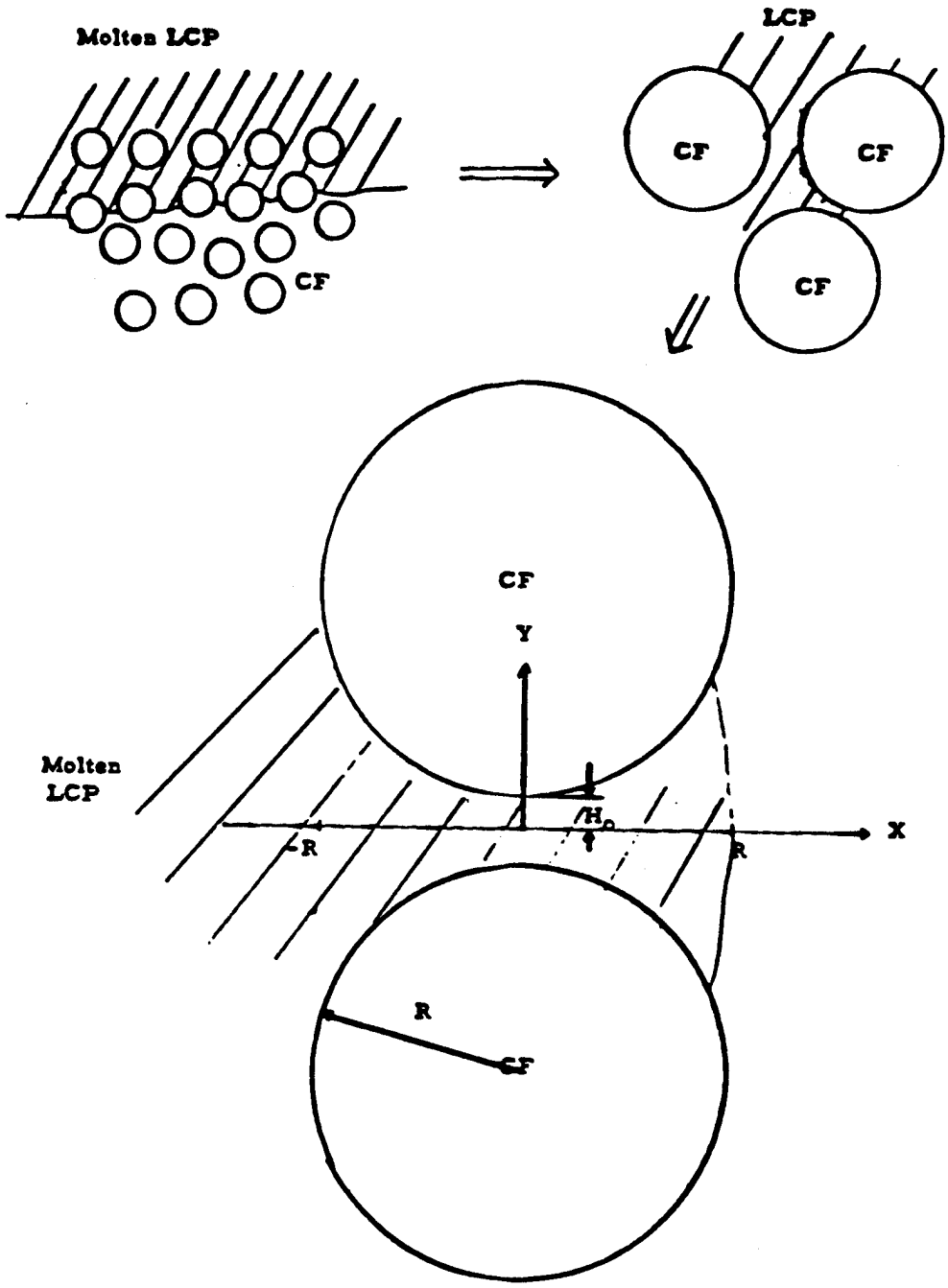


FIGURE 1. IMPREGNATION OF LCP INTO CF BUNDLE

On the other hand, if the fiber and the matrix have poor interfacial attraction, the maximum pressure needed to overcome the poor wetting character may be derived as (31):

$$\Delta P_2 = \frac{\gamma}{R\cos\theta + \sqrt{(R+Ho)^2 - R^2\sin^2\theta}} \qquad (2)$$

where $\gamma$ is the surface tension, $\theta$ is the advancing fiber contact angle. (Figure 2 demonstrates the schematic diagram of fiber-wetting process.) Figures 3 and 4 show the calculated results for equations (1) and (2), respectively. Comparing these, we can make the following conclusions:

1. For large Ho/R, the effects of the rheological behavior and the advancing contact angle on the penetration of LCP into fibers are comparable. If the contact angle is high and viscosity is low, the influence of the contact angle (or sizing) is very significant.
2. For low Ho/R, the effect of the rheological behavior becomes a dominant factor for the impregnation, especially when $\theta$ <90°.
3. In the epoxy matrix system, the surface tension is generally a dominant factor. This is because the viscosity of epoxy is 15 to 100 times lower than that of thermoplastic matrix polymers.

Therefore, the following approaches may be useful to improve fiber wet-out.

1. Increase process pressure by a closed system.
2. Decrease melt viscosity by changing material fluid behavior (polymer, temperature).
3. Reduce melt surface tension by changing material properties.
4. Reduce contact angle by modifying fiber sizing.

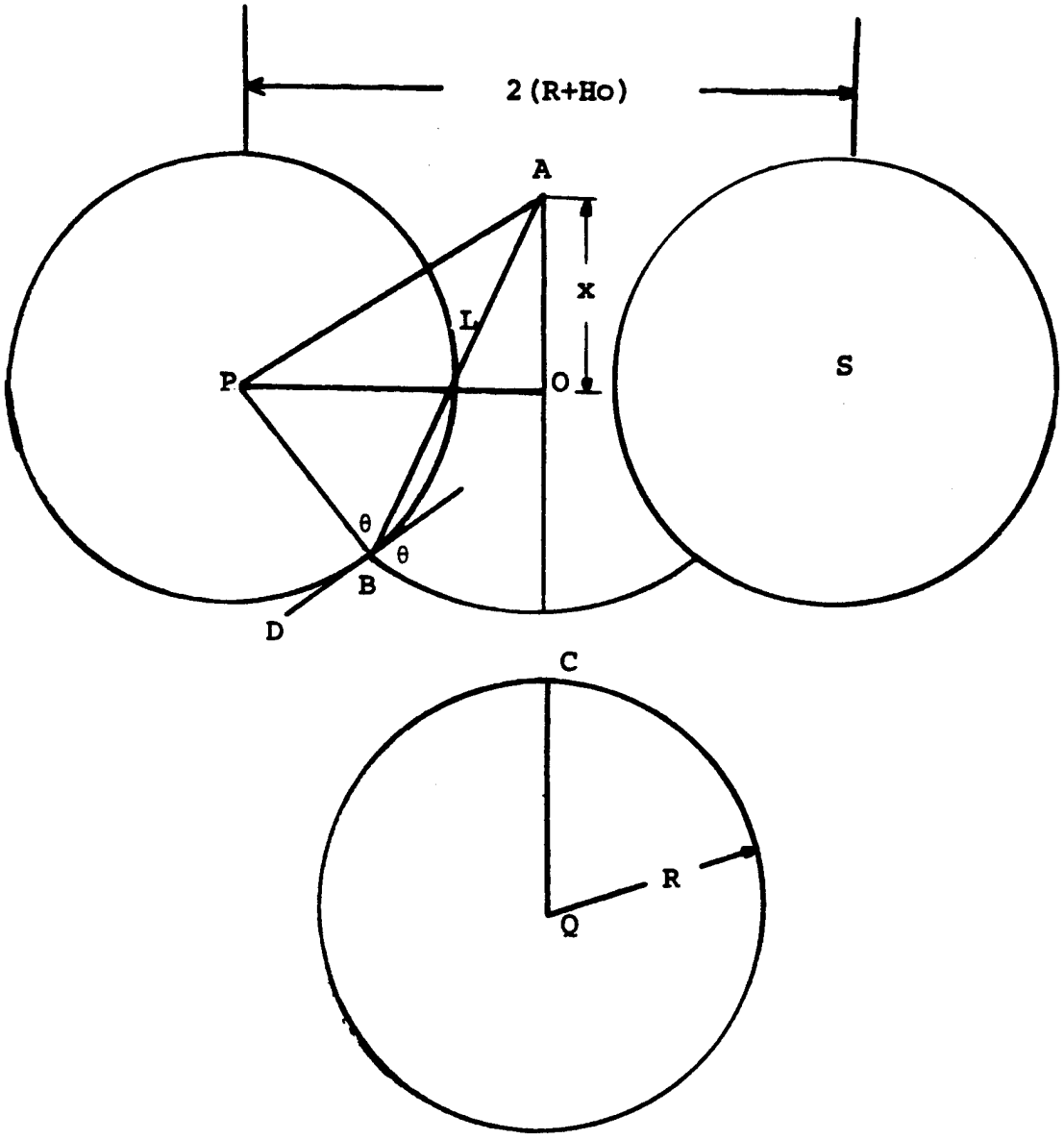


FIGURE 2. PENETRATION OF LCP BETWEEN FIBER CYLINDERS

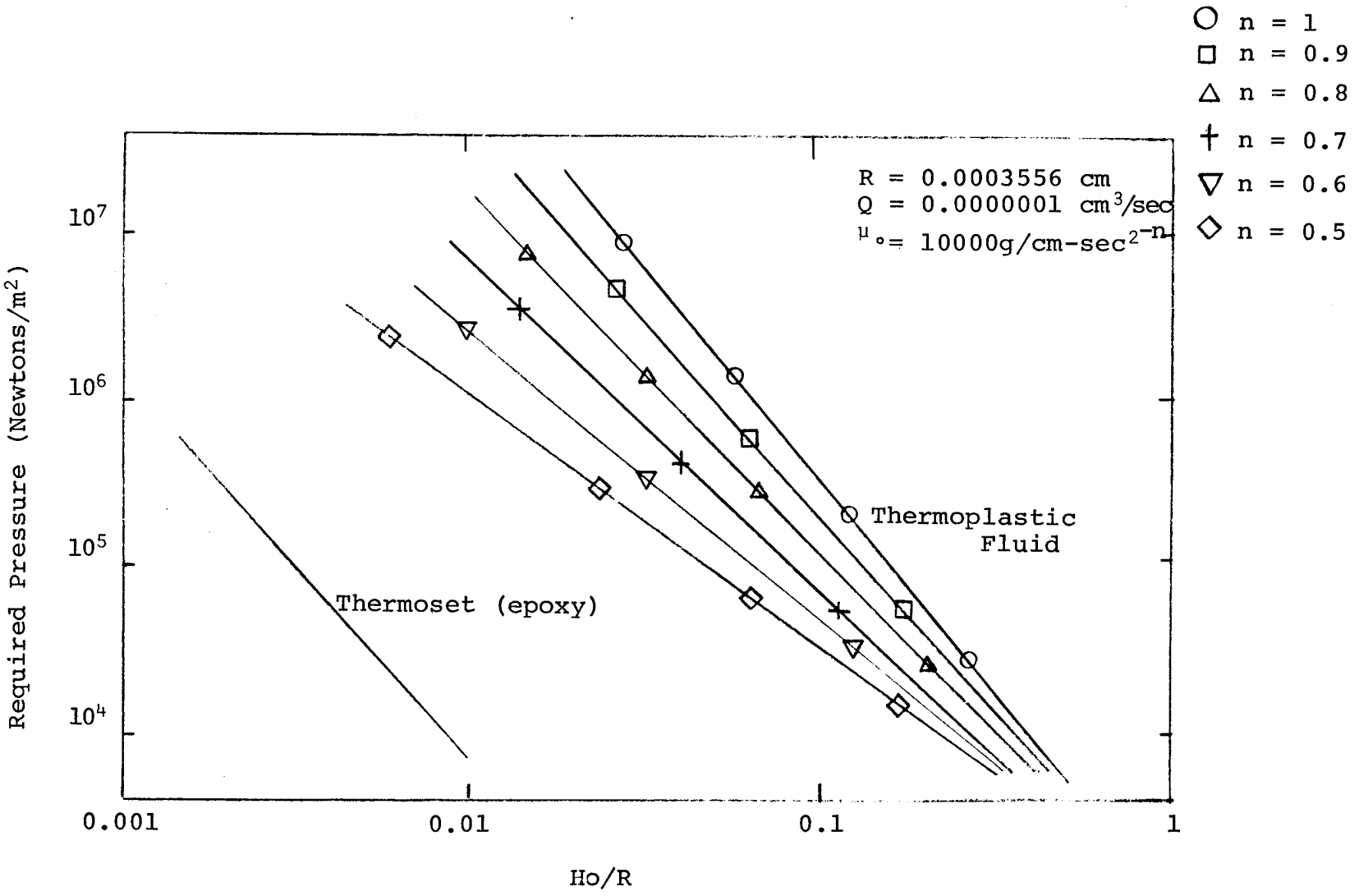


FIGURE 3. REQUIRED PRESSURE DROP vs Ho/R

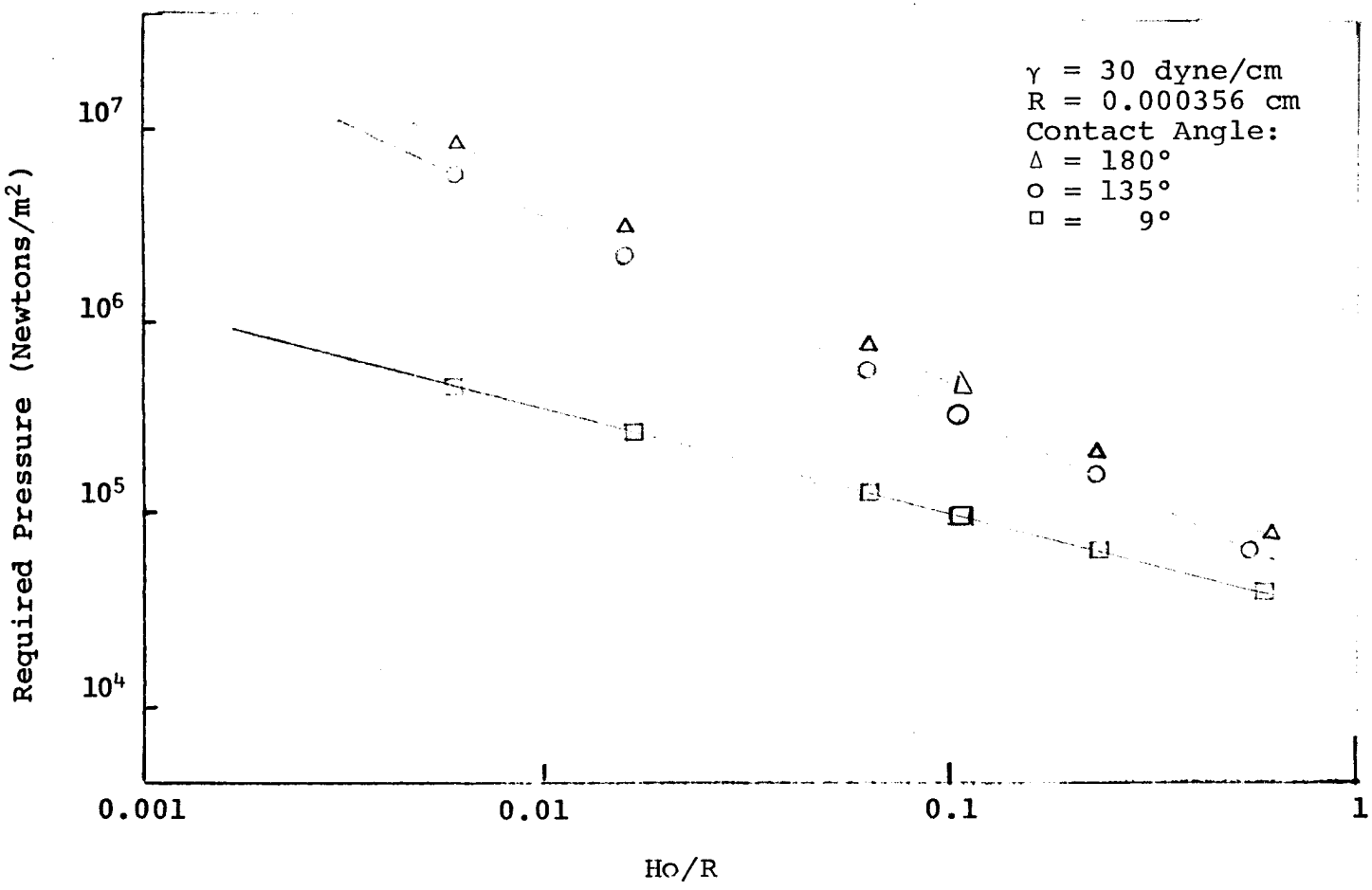


FIGURE 4. REQUIRED PRESSURE DROP vs Ho/R

5. Reduce CF filament diameter.
6. Increase distance between CF filaments.

Since it is impossible to significantly increase process pressure in a continuous pultrusion process, finding a way to change melt character and reduce contact angle involves a complicated research program. A reduction of fiber diameter is not easy because it may create other problems. The best approaches to meet our target are in the second and sixth choices. Therefore, in this report we have chosen a liquid crystal polymer with low melt viscosity at high temperatures and have developed techniques to increase the distance between fibers by a variety of mechanical approaches.

## SECTION 4. MATRIX CHARACTERISTICS

### 4.1 Polymer Formation and Melt Characterization

The material studied is an all aromatic copolyester of 2,6-hydroxynaphthoic acid, terephthalic acid, and 4'-hydroxyacetanilide. This polymer was invented by East et al, and the details of polymerization conditions were described in the patent.[32] Figure 5 shows its chemical structure. The polymer is a high molecular weight copolyester, and exhibits ordered structure in the melt, as indicated by birefringent optical properties. Figure 6 demonstrates its melting behavior as determined by differential scanning calorimetry using a 20°C/min heat-up rate. This figure shows that the polymer has a very broad softening and gradual melting behavior from about 220°C up to about 290°C. The very small endotherm implies that the three-dimensional crystallinity of the LCP is not very high. Upon cooling, a small crystallization peak shows at 230-236°C at 20°C/min cooling rate. The polymer has an inherent viscosity of approximately 4.5 dL/g. Figure 7 shows the melt viscosity as a function of shear rate and temperature. This polymer has much lower viscosity than most of the conventional thermoplastic polymers.

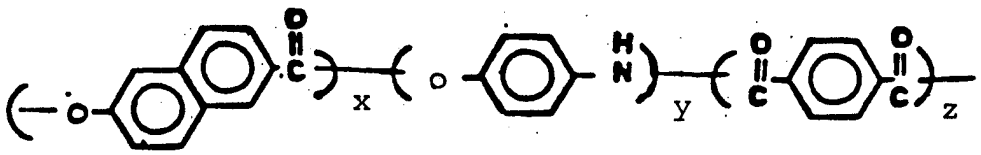

FIGURE 5. CHEMICAL STRUCTURE OF LIQUID CRYSTAL POLYMER

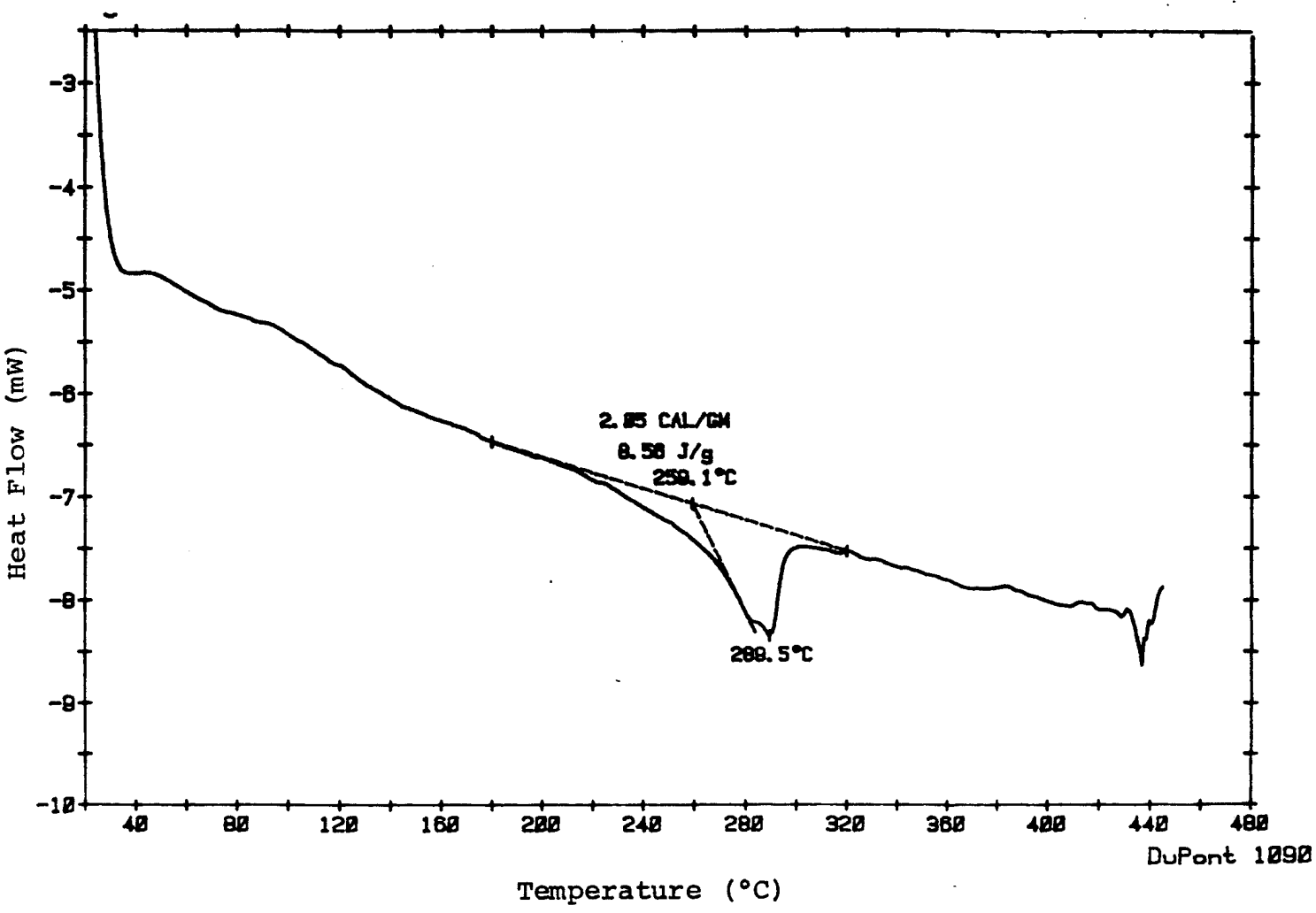


FIGURE 6. THE DSC CURVES OF LCP FILM

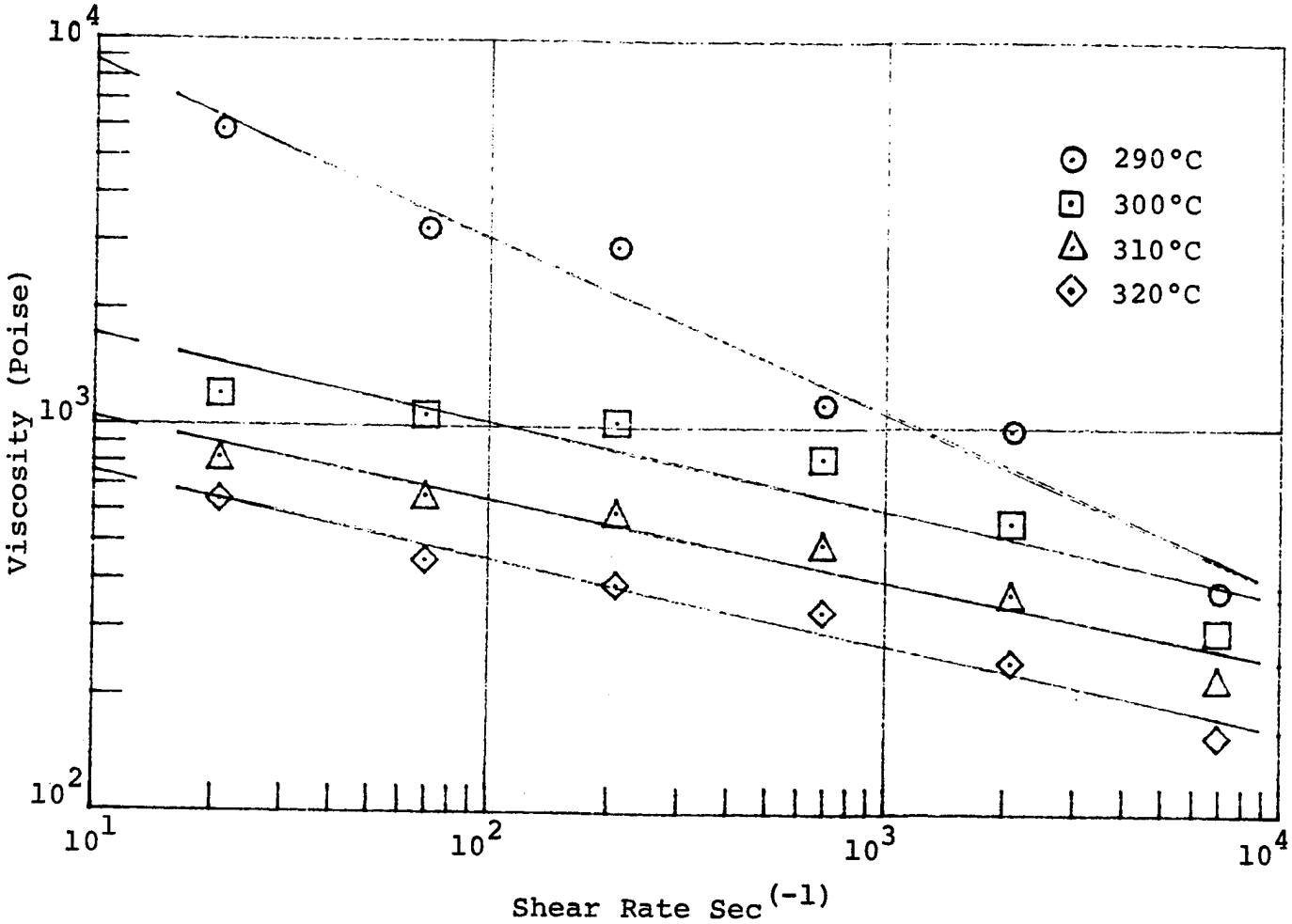


FIGURE 7. VISCOSITY OF LCP AS A FUNCTION OF SHEAR RATE AND TEMPERATURE

## 4.2 Polymer Tensile Properties and Chemical Resistance

The tensile properties of the neat resin in different environmental conditions are shown in Table 1. The chemical resistance to Skydrol® and methylene chloride is excellent.

Dynamic mechanical analyses of as-extruded strands were conducted at temperatures ranging from -120°C to 240°C. Figure 8 shows the results and indicates that the modulus is highest at cryogenic conditions, but it drops sharply at both the $\beta$ transition (between 20°C and 70°C) and the $\alpha$ transition (140°C).

## 4.3 Crack Propagation Measurements ($K_{1c}$)

The critical stress intensity factor of neat resin was determined by measuring the Mode 1 fracture toughness, $K_{1c}$, of injection molded LCP plaques. Because the injection gate was located on the peripheral edge of the molded disk, it produced an anisotropic flow field. Two measurements were made parallel to the machine direction (designated longitudinal) and four in the direction perpendicular to the flow from the gate (designated transverse).

Specimens were fabricated to the geometry specified in Figure 9. Load was introduced into the specimen through 1.27 cm (1/2 in) pins inserted through a clevis arrangement mounted in a standard TTC Instron test machine. A schematic of the test set-up is shown in Figure 10. Precracking was performed by shaping a notch with 45° angle and with a load-point displacement rate of 0.05 cm/min until a crack propagated a short distance from the line of action. Then load was applied by moving the cross-head at a constant rate of displacement until the crack in the specimen began to propagate as indicated by a drop in load recorded on the load displacement curve. At this point the test is stopped, the specimen unloaded and a measurement taken of the new crack length. The load at which the crack of length $a_i$ begins to propagate is designated $f_i$ and used to determine $K_{1c}$ for that given

---

Skydrol® is a registered trademark of Monsanto Corporation.

TABLE 1. TENSILE PROPERTIES OF INJECTION MOLDED LCP 4060 AT ROOM TEMPERATURE

| Conditioning | % Weight Gain | Tensile Strength (MPa) | (Ksi) | Tensile Modulus (GPa) | (Msi) |
|---|---|---|---|---|---|
| Control | - | 162.1 | (23.2) | 23.5 | (3.36) |
| 140°F/98% RH (30 days) | 0.036 | 141.1 | (20.2) | 22.4 | (3.20) |
| $CH_2Cl_2$ (30 days) | -0.023 | 176.8 | (25.3) | 24.7 | (3.53) |
| Skydrol (30 days) | 0.018 | 174.7 | (25.0) | 21.0 | (3.00) |

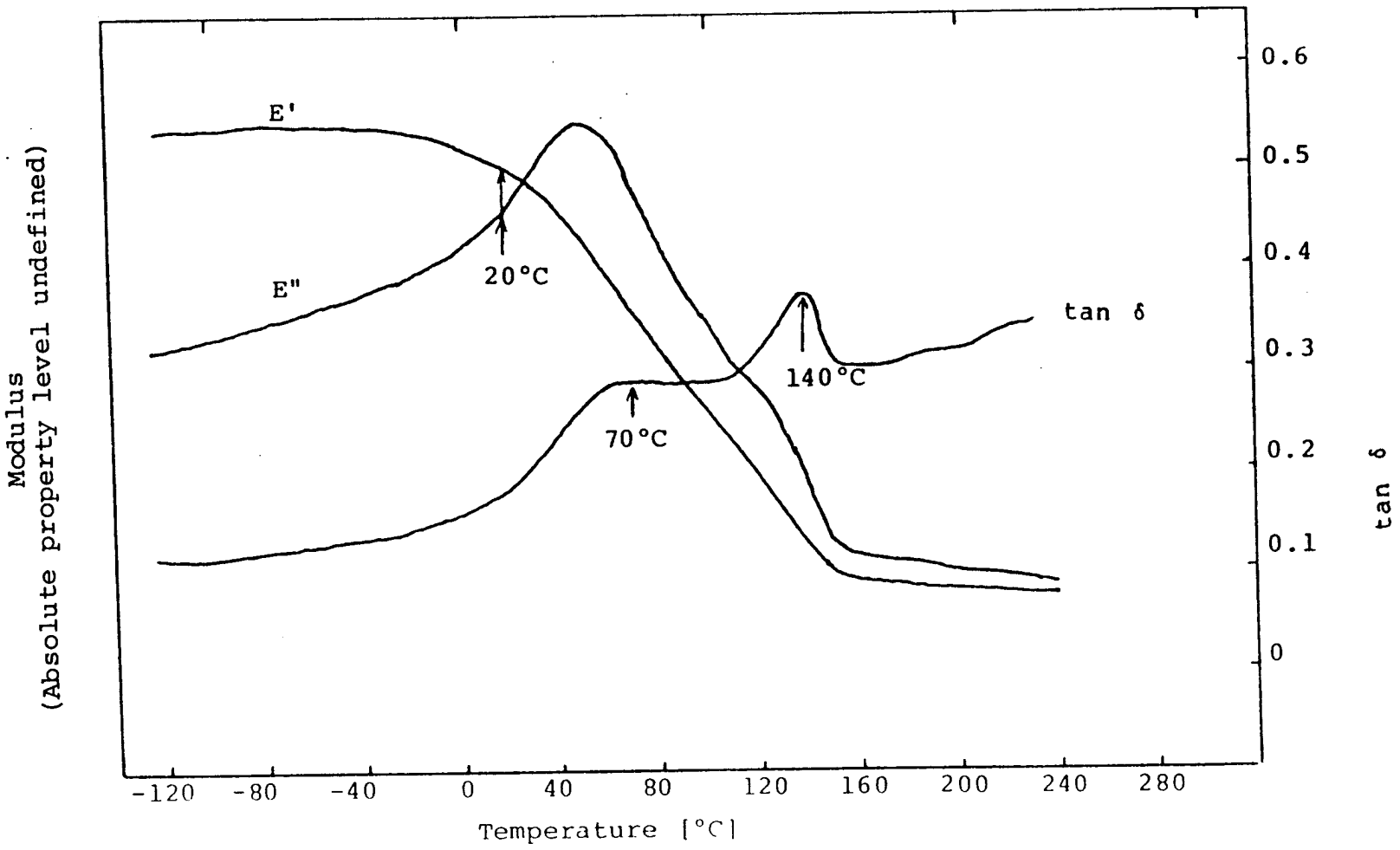


FIGURE 8. DMA CURVE OF AS-EXTRUDED LCP STRAND

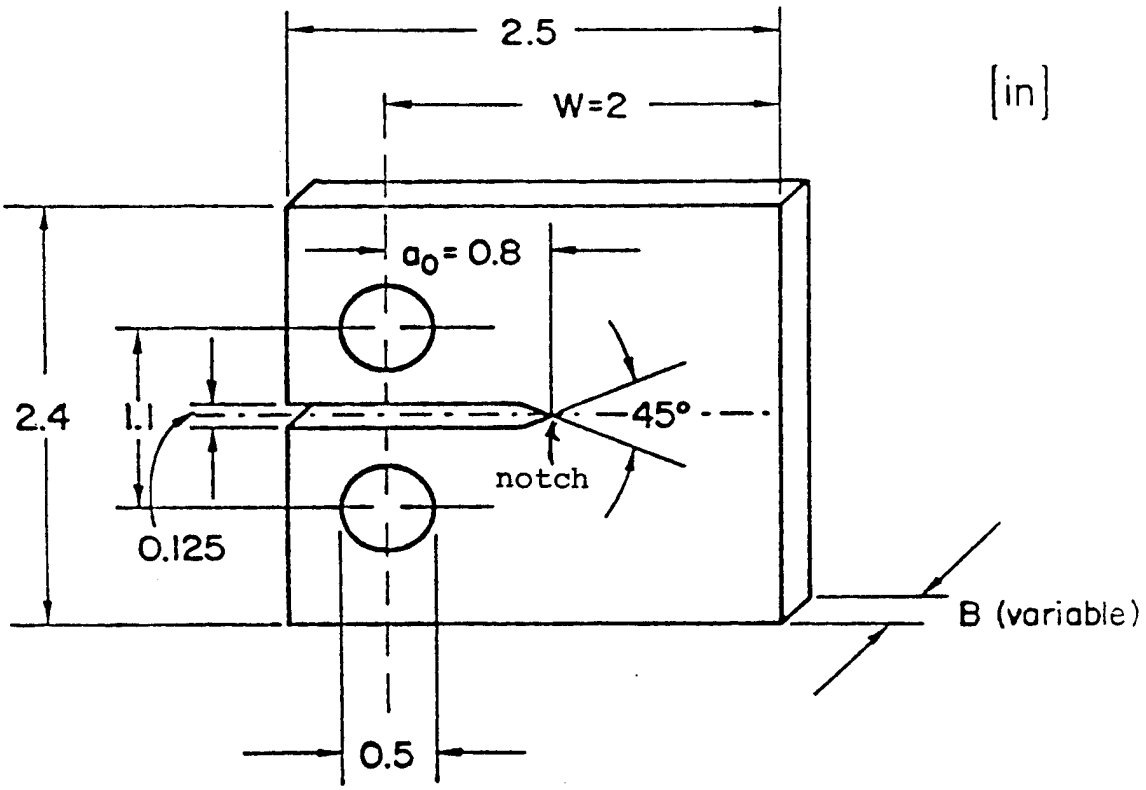


FIGURE 9. COMPACT TENSION SPECIMEN CONFIGURATION

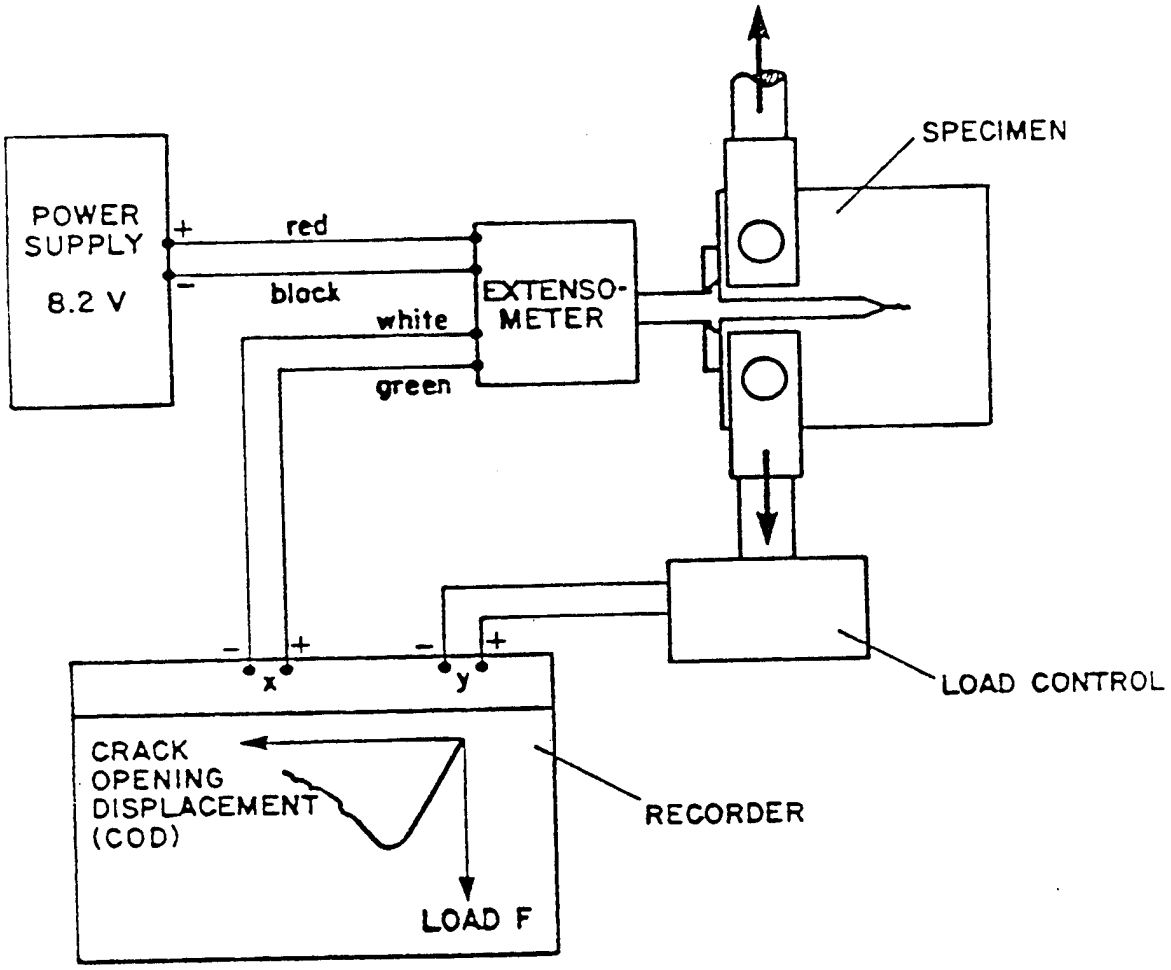


FIGURE 10. BLOCK DIAGRAM OF LOAD-CRACK OPENING DISPLACEMENT MEASUREMENTS

crack length. Crack lengths of the "natural cracks" were determined by averaging the measured length on each surface of specimen. "Natural cracks" are defined as cracks whose crack front is the result of a previous propagation event, not a machining operation. The calculation of $K_{1c}$ employs the following relationship:

$$K_{1c} = \frac{f_i}{B\ W^{1/2}} \cdot Y(a_i\ W)$$

where:

$f_i$ = propagation load

$B$ = thickness

$W$ = width

$a_i$ = crack length

$Y(a_i/W)$ = geometric correction factor

and:

$$Y(a_iW) = 29.6(a_i/W)^{1/2} - 185.5(a_i/W)^{3/2} + 655.7(a_i/W)^{5/2} - 1017(a_i/W)^{7/2} + 638.9(a_i/W)^{9/2}$$

The test procedure is repeated on a single specimen for several crack lengths, usually about four. When the crack gets to within 1.27 cm (0.5 in) of the specimen's edge, no further data are taken due to the influence of the edge on the measurements. Figure 11 presents the results for the longitudinal measurements from specimens specified as L1 and L3. The relatively high scatter is typical of this type of test applied to polymeric and fiber reinforced materials. The solid line indicates the average $K_{1c}$ determined from natural crack data only and the dashed line the average $K_{1c}$ including all data points. For these specimens, the crack propagation was dominantly co-linear with the starter crack, but wandered slightly (see Figure 12). This

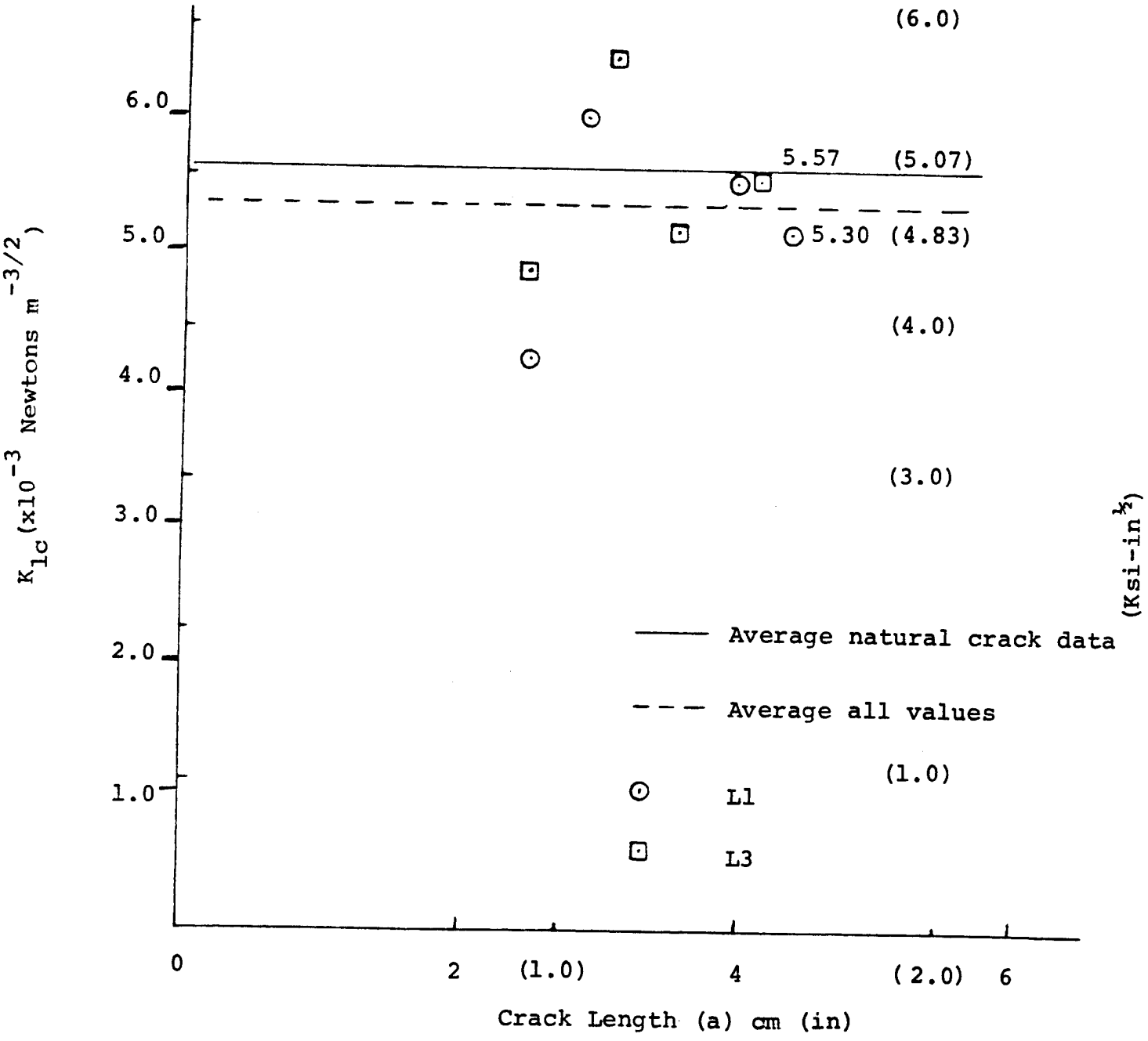


FIGURE 11. $K_{1c}$ VS CRACK LENGTH FOR LONGITUDINAL SPECIMENS

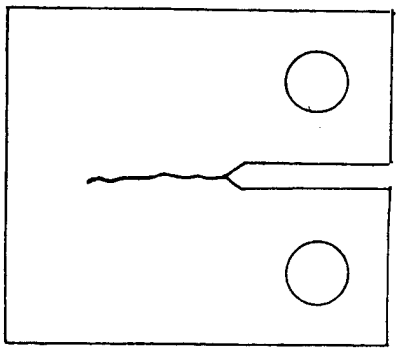

Longitudinal

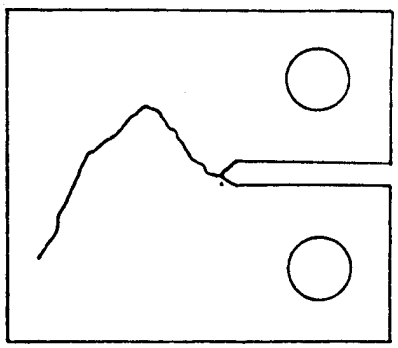

Transverse

FIGURE 12. CRACK PROPAGATION CHARACTERISTICS FOR LONGITUDINAL AND TRANSVERSE SPECIMENS

slight amount of wandering accounts for most of the variability in the data.

Results for the transverse specimens are shown in Figure 13. In these specimens the crack did not propagate co-linearly with the machined crack. A typical crack path is shown in Figure 12. Under these circumstances, the $K_{1c}$ calculations are significantly in error. Therefore, the data presented in Figure 13 is not a valid quantitative measure of $K_{1c}$ in the transverse direction of the material. Again the averages are shown based on natural crack data (solid line) and all data (dashed line) but these numbers are probably lower than the actual $K_{1c}$.

From a basic standpoint of mechanics, the relationship between the $K_{1c}$ and the energy release rate is:

$$G_{1c} = \frac{K_{1c}^2}{E}(1-v)$$

where E is Young's modulus and v is the Poisson's ratio. Since the tensile modulus of LCP is much higher than most conventional thermoplastics and thermosets, this equation implies that the fracture toughness of this LCP may be lower than other less ordered thermoplastics. This deficiency may arise from the fact that the highly oriented LCP molecules lead to poor inter-lamina cohesion.

## SECTION 5. FABRICATION PROCESS

### 5.1 Prepreg Line

The impregnation was carried out in a cross-head tape die, designed for 3" wide tape as illustrated in Figure 14. Molten LCP polymer was supplied by a twin screw extruder to the channels of the tape die. The extruder has three temperature controllers to monitor the temperature profiles at feeding, transition and metering zones. In these experiments, these three controllers were set at 290°C. The cross head die was set at 320°C. Ten to

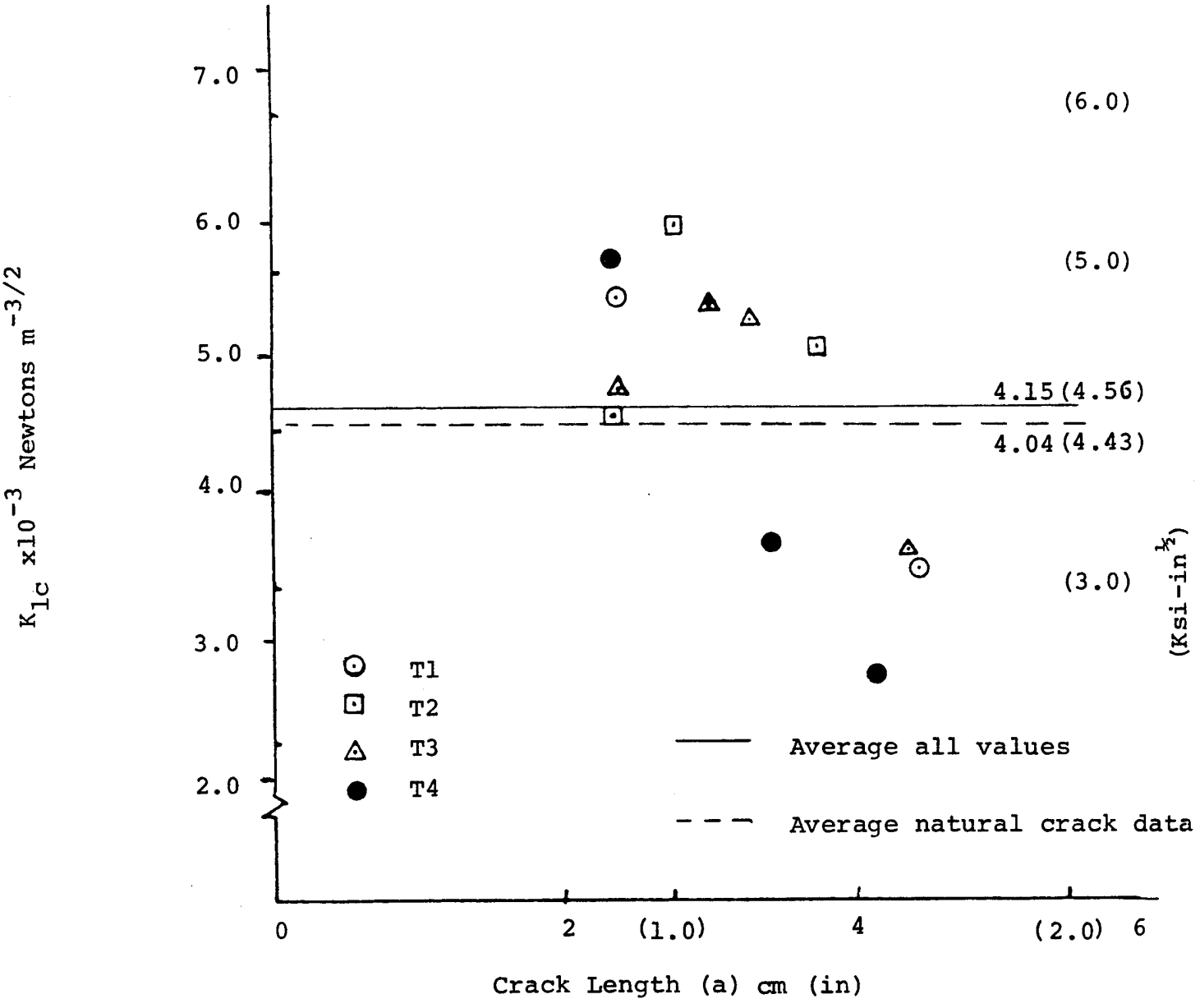


FIGURE 13. $K_{1c}$ VS CRACK LENGTH FOR TRANSVERSE SPECIMENS

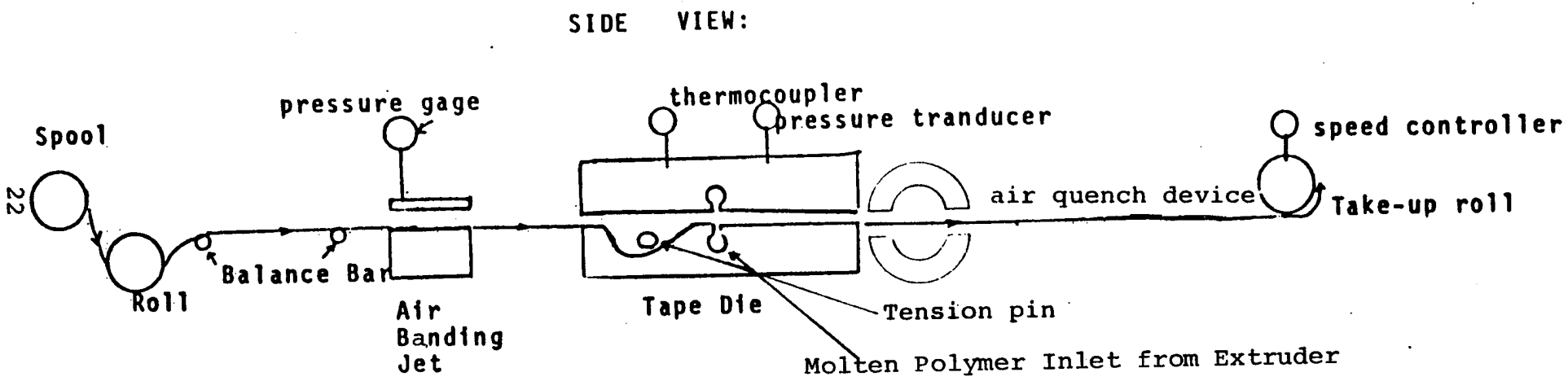


FIGURE 14. SCHEMATIC DIAGRAM OF PREPREG LINE

twenty ends of unsized Celion® 6000 carbon fiber could be pulled horizontally through the die at speeds ranging from inches per minute to 10 feet per minute. Experimental results indicated that pultrusion of ten ends 6K at 0.5 cm/sec is the best condition. Flex lips were placed at the entrance and exit to generate high polymer pressure. The melt chamber and a built-in tension pin in the tape die give better fiber alignment and have longer residence time for melt impregnation. Tapes produced via this process had 40-55 volume % fiber loading, fair wet-out and good fiber alignment. Their thicknesses varied from 0.007 to 0.012 cm. The wet-out of tape generally was controlled by many parameters. It was found that the wet-out of tape was improved at higher tape temperatures. This is in agreement with our theoretical predictions. However, if the die temperature is higher than 350°C, the LCP melt starts to degrade and discolor. If the die temperature is lower than 300°C, the wet-out is very poor and LCP matrix coats both sides of tape without impregnation within the bundle.

It was observed that the fiber exits from the cross-head tape die with an even distribution of bundles and filaments, but this distribution is distorted almost immediately due to the fluidity of the thermoplastic melt as well as the tension imposed by the take-up roll. As a result, pockets of polymer or air voids were left trapped between the fiber bundles. Many approaches have been used in order to overcome this problem. A single nip roll was installed after the crosshed die; however, the roll temperature changed and therefore caused sticking of the polymers on the rolls. Another approach is to increase the number of fiber ends but reducing the fiber wet-out. Finally, this problem was resolved by inventing an air quench device which causes quick setting of the polymer melt immediately after exiting the cross-head tape die. This quick quenching restricts the carbon fibers from moving and yields a uniform carbon fiber distribution across the matrix resin in the prepreg.

---

Celion is a registered trademark of the Celanese Corporation.

## 5.2 Panel Preparation

Carbon fiber/LCP resin composite panels were prepared by compression molding of the tapes. This compression molding process is shown in Figure 15 and utilized a Carver laboratory press, a 50 ton hydraulic press and a highly polished 8.9 cm x 26.5 cm rectangular mold. Heating elements were installed in the Carver press and their temperature was monitored by a temperature controller in each platen. The process is therefore capable of molding panels at specific temperature and pressure conditions. The thickness of fabricated panel was controlled by the number of tape plies inserted into the mold for compression molding. The tight tolerances on the mold allowed pressure in excess of 6.9 x $10^6$ $N/m^2$ (100 psi) with little polymer leakage. Usually, panels were compression molded at 300-340°C under a pressure of 7-35 x $10^5$ $N/m^2$ (100-500 psi) for 10-15 minutes in the hot Carver press and then transferred to a cold hydraulic press for cooling. The pressure during the cooling stage was about 6.9 x $10^6$ $N/m^2$.

## 5.3 Vacuum Bag

Minimum voids content in composites is essential for maximizing mechanical properties. Without applying vacuum to the lay-up of plies prior to compression molding, air was trapped between the various plies and caused a greater than desirable void content in the composite panel. By wrapping the ply assembly with a high temperature resistant Kapton film and applying vacuum, we successfully reduced void content in the composite panel to <0.8% by volume (density measurement).

Figure 16 shows a scanning electron micrograph of a cross section of a compression molded carbon fiber (Celion® 6000, unsized) LCP panel and clearly illustrates a good fiber/resin distribution.

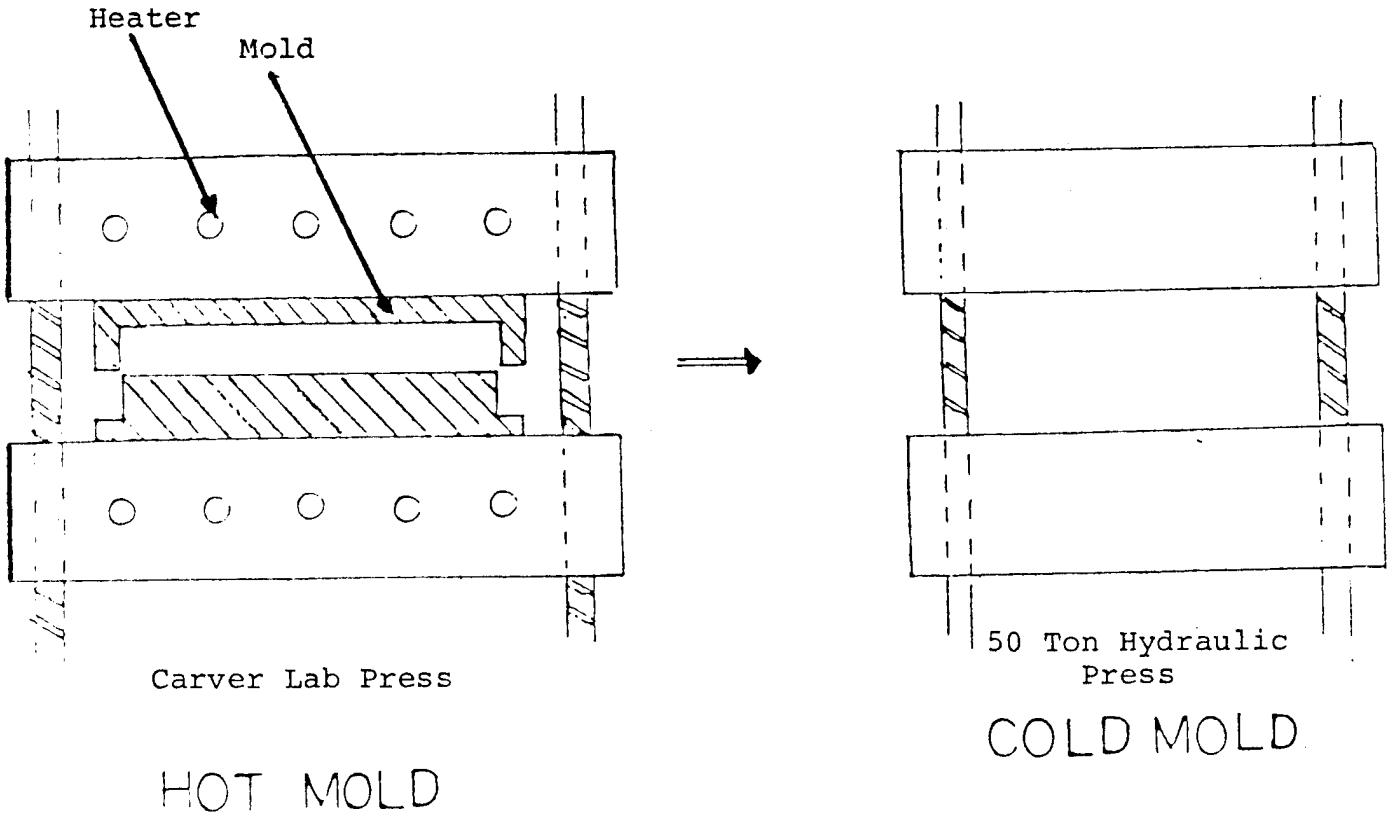


FIGURE 15. ARRANGEMENT FOR COMPRESSION MOLDING PROCESS

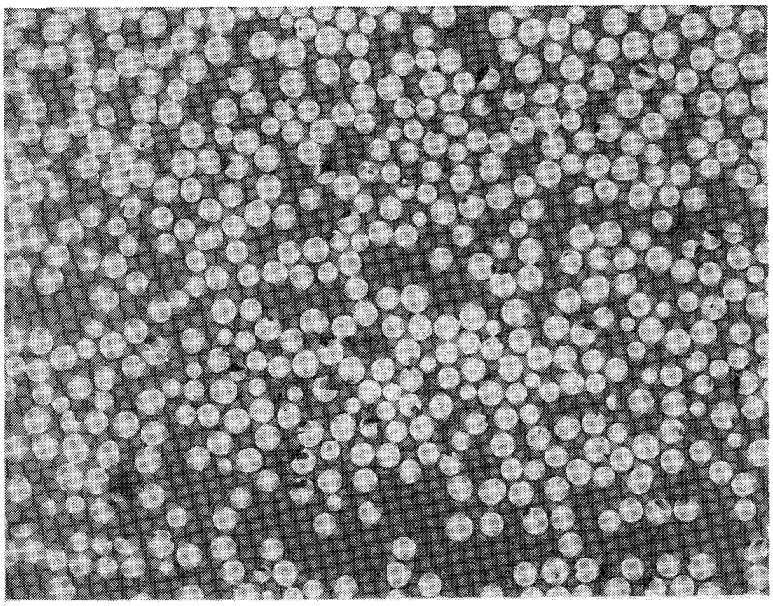

500X

FIGURE 16. SCANNING ELECTRON MICROGRAPH OF A CROSS SECTION OF LCP CARBON FIBER COMPOSITES (57 VOLUME %)

## 5.4 Test Specimen Preparation

The mechanical properties of the molded panels were determined using the following ASTM methods; D3039 for tensile properties, D790 for flexural properties and D2344 for shear properties. Specimens were prepared with 0° carbon fiber orientation. Flexural strength and modulus were measured using a 3-point flex test and approximately 32:1 span-to-depth ratio, while short beam shear strength used a 4:1 span-to-depth ratio. Compression properties were measured using compression fixture developed by Celanese where test specimens were 0.20 cm thick, 0.635 cm wide and 10.8 cm long. Tensile specimens were 1.27 cm wide and 21.59 cm long. Four glass fiber tabs, 1.27 cm wide and 5.72 cm long, were mounted on specimens prior to testing. Forty-five degree tensile strength samples were fabricated using $(45°/-45°)_{3S}$ lay-up. Test samples were 2.54 cm wide and 22.86 cm long and were mounted with four 2.54 cm wide and 5.08 cm long glass fiber tabs. Open hole tensile samples were laminated employing $(45/90/-45/0)_{2S}$ sequence. Test specimens were 3.81 cm wide and 22.86 cm long and a hole with 0.635 cm diameter was drilled through the center of the flat specimens. The deflection rate during testing was 0.127 cm/min. Impact measurements were also made on samples employing a $(45/90/-45/0)_{2S}$ lay-up.

## 5.5 Mechanical Properties of LCP/CF Composites

Tensile and flexural properties of LCP/CF composites are given in Tables 2 and 3. The wet term "Conditions" in Tables 2 and 3 means that the samples were immersed in water at 160°F for two weeks and then tested at the temperature indicated. Both tensile and flexural properties are comparable to commercial epoxy/CF composites at the same volume content of carbon fiber. Flexural modulus retention at elevated temperatures is extremely good. However, the flexural strength retention at 200°F is fair (67%) and becomes poor (54%) if the test temperature is at

TABLE 2. TENSILE PROPERTIES OF UNIDIRECTIONAL LCP 4060/CF COMPOSITES

| CF Volume % | Conditions | Tensile Strength MPa (Ksi) | Tensile Modulus GPa (Msi) | Tensile Strain % |
|---|---|---|---|---|
| 56.5 | Dry | 1492 (217) | 143 (20.7) | 1.045 |
| 56.5 | Wet | 1297 (188) | 121 (17.6) | 1.071 |

TABLE 3. FLEXURAL PROPERTIES OF LCP 4060/CF UNIDIRECTIONAL COMPOSITES

| Fiber Content (V%) | Conditions | Flexural Strength MPa(Ksi) | Flexural Modulus GPa(Ksi) |
|---|---|---|---|
| 51 | RT (dry) | 1515(220) | 106.5(15.45) |
| 51 | RT (wet) | 1447(210) | 106.0(15.39) |
| 51 | 200°F(dry) | 1054(153) | 106.2(15.42) |
| 51 | 200°F(wet) | 904(140) | 105.3(15.28) |
| 51 | 250°F(dry) | 744(108) | 98.8(14.34) |
| 51 | 250°F(wet) | 854(124) | 97.8(14.19) |

250°F. This poor retention may be due to two factors: (1) the low β-transition of LCP at 158°F; and, (2) a poor interface between fiber and matrix. Thus, the adhesion between fibers and matrix failed long before the composites fails resulting in slip near the fiber ends.

Tables 4 and 5 summarize the shear strength and compression properties of LCP/CF composites. Both room temperature shear and compression strength are inferior to the epoxy/carbon fiber composites. The temperature retention of shear strength is inferior to the epoxy/carbon fiber composites. The temperature retention of shear strength at elevated temperatures is also poor. Compression samples failed through fiber buckling and composite delamination. Figures 17 and 18 show SEM micrographs of the fracture (fiber buckling) and delamination surfaces of a tested compression sample. Figure 17 clearly indicates that every fiber has been surrounded with matrix, but adhesion between them is poor. Figure 18 demonstrates that fibers have good alignment but poor interfacial adhesion. Therefore, the poor compression and shear strength may be attributed to poor interface adhesion between unsized carbon fiber and LCP matrix as well as poor intermolecular cohesion within the LCP polymer.

The mechanical properties of an isotropic cross-laminated lay-up panel are given in Table 6. Both open hole and $\pm$ 45° tensile strength are comparable to epoxy/carbon fiber composite properties. Impact test results indicate that the isotropic panel has a maximum load of 2420 Newtons which is clearly superior to thermoset matrix systems (typically 1480 Newtons).

TABLE 4. SHORT BEAM SHEAR STRENGTH OF UNIDIRECTIONAL LCP 4060/CF COMPOSITES

| Fiber Content (V%) | Conditions | Shear Strength MPa | (Ksi) |
|---|---|---|---|
| 58 | RT | 52 | (7.6) |
| 58 | 200°F | 37 | (5.4) |
| 58 | 250°F | 23 | (3.9) |

TABLE 5. COMPRESSION PROPERTIES OF UNIDIRECTIONAL LCP 4060/CF COMPOSITES

| V% | Conditions | Compression Strength MPa(Ksi) | Modulus GPa(Msi) |
|---|---|---|---|
| 45 | RT | 809(117.5) | 117(17) |
| 50 | RT | 862(125.0) | 120(17.5) |

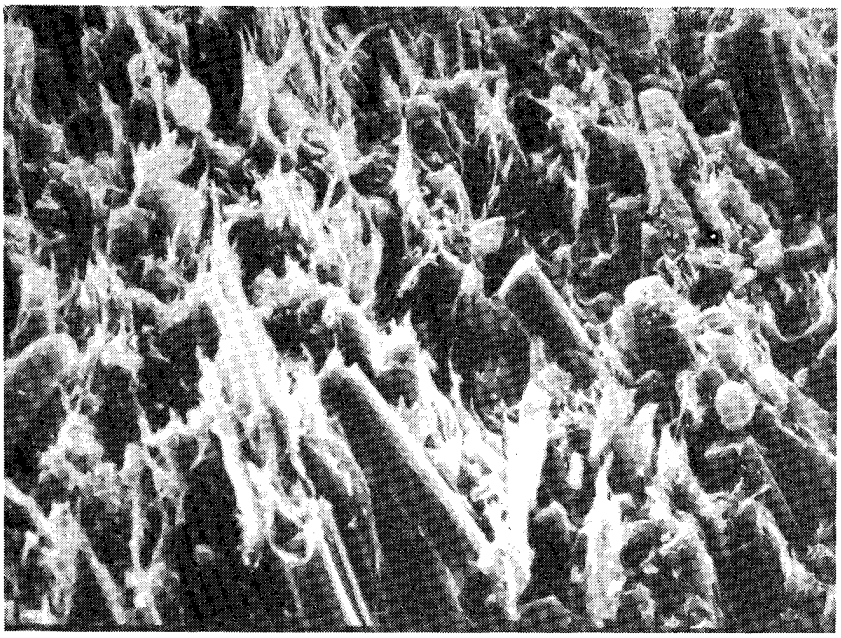

FIGURE 17. FRACTURE SURFACE OF A COMPRESSION SAMPLE

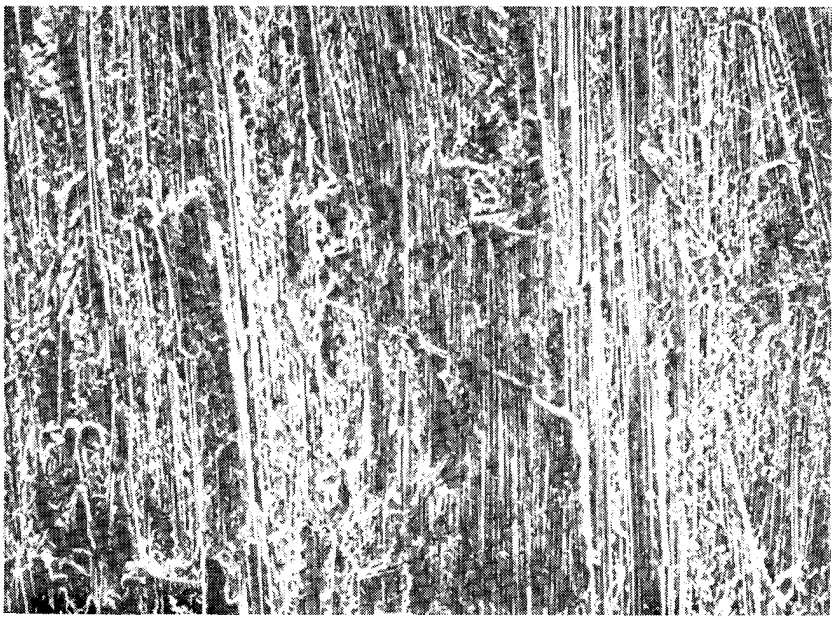

FIGURE 18. DELAMINATION SURFACE OF A COMPRESSION SURFACE

TABLE 6. MECHANICAL PROPERTIES OF ISOTROPIC LAMINATED PANEL

| Property | CF Volume % | Result |
|---|---|---|
| Open Hole Tensile Strength | 52 | 313.5 MPa (45.5 Ksi) |
| 45° Tensile Strength | 53 | 134.5 MPa (19.5 Ksi) |
| Impact Test: | | |
| Max. Load | 52 | 2420 Newtons (740 lb) |
| Energy at Max. Load | 52 | 2.76 Joules (2.04 ft-lb) |

## SECTION 6. MANIPULATION OF LCP MOLECULAR ORIENTATION

### 6.1 Sample Preparation

As stated in the introduction, the surface chemistry of carbon fibers may influence the structure of a thermoplastic matrix. Our studies have therefore investigated the orientation behavior of LCP on carbon fiber surface.

Composite panels were fabricated by interweaving spread unidirectional spread carbon fiber ends with extruded unidirectional LCP film (2 mil thickness). Figure 19 illustrates the process where LCP film was mounted on a drum and carbon fiber bundles were spread by an air banding jet. Due to the highly anisotropic nature of the thermotropic melt and the orientation induced by extrusion process, the 2 mil liquid crystal film has significant property anisotropy between the extrusion and transverse directions as shown in Table 7. Therefore, two types of layouts were prepared; one with original LCP film orientation parallel to the carbon fiber direction, and the second one with original film orientation perpendicular to carbon fiber direction. In order to prevent the movement of fibers on the LCP sheet, samples were carefully removed from the drum and covered by a Kapton® film. These were then immediately placed on a hot plate at 550°F for one minute. A slight pressure was applied on the prepreg in order to consolidate the fibers and LCP sheet together. Thirty samples of these prepregs were then compression molded under the same conditions described in Section 5.2.

### 6.2 X-Ray Measurement

The orientation of LCP matrix and carbon fiber in molded panels was examined using x-ray diffraction. For this study, the following coordinate axes are defined (for reference, see Table 8):

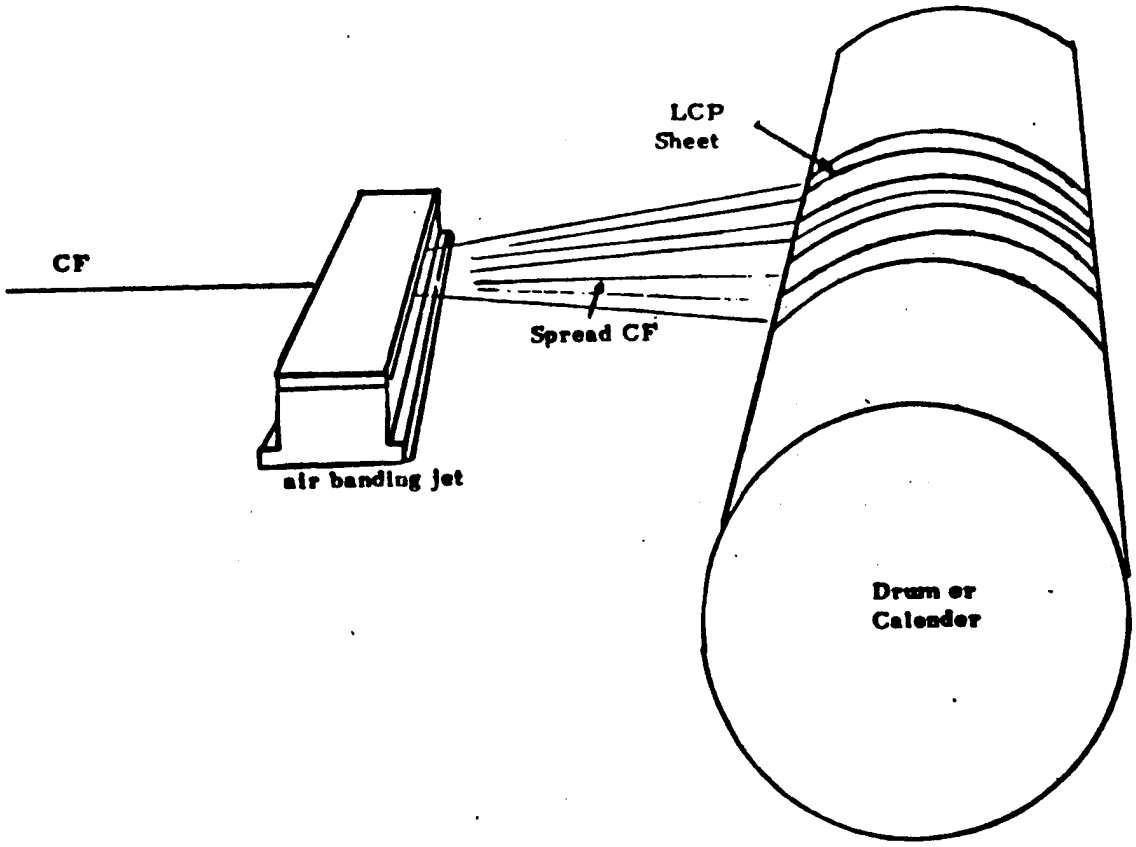


FIGURE 19. SHEET PROCESS

TABLE 7. TENSILE PROPERTIES OF LCP FILM

| | Tensile Strength MPa | (ksi) | Tensile Modulus MPa | (Msi) | Elongation % |
|---|---|---|---|---|---|
| Machine Direction | 550 | (79.7) | 18 | (2.60) | 4.49 |
| Transverse Direction | 14.6 | (2.11) | 0.83 | (0.12) | 1.94 |

X = parallel to the carbon fiber axis and parallel to the composite panel surface (longitudinal direction);

Y = perpendicular to the carbon fiber axis and parallel to the composite panel surface (width direction);

Z = perpendicular to the carbon fiber axis and perpendicular to the composite panel surface (thickness direction).

Diffraction patterns were recorded photographically using nickel filtered CuK$\alpha$ radiation with the incident beam aligned along each of the above directions. Orientation parameters were computed from digitized azimuthal microdensitometer scans of the <002> carbon fiber reflection, or the <110> liquid crystal polymer reflection, both of which occur in a plane perpendicular to the fiber or molecular axis, respectively. Herman's orientation functions were calculated assuming uniaxial orientation from these strong equatorial reflections for both the carbon fiber and the liquid crystalline polymer components. Uniaxial orientation was verified by x-ray diffraction patterns obtained with the incident beam directed along the X axis. The equatorial nature of each reflection was taken into account so that the Herman's orientation function is defined, as usual, by:

$$f = \frac{3\langle\cos^2\theta\rangle - 1}{2}$$

where $\theta$ is the angle between the polymer axis (or the carbon basal plane) and the fiber axis, and where the brackets indicate average overall molecules (or carbon basal planes). $\theta$ is not directly measured, but $\langle\cos^2\theta\rangle$ is computed from the azimuthal angular distribution of intensity for each equatorial reflection obtained from patterns for which the incident x-ray beam is directly along the Y or Z axis.

## 6.3 Results and Discussion

Figure 20 illustrates typical x-ray diffraction patterns of a Celion® carbon fiber and a liquid crystal polymer. The angular width (full width at half integral intensity) of the equatorial <002> reflection was 21.4° for the carbon fiber and 8.2° for the <110> from the highly oriented LCP films. Fabrication of carbon fiber and LCP films with 0° and 90° orientation between the uniaxial carbon fiber and LCP axes supposedly yields panels where carbon fiber and LCP should remain parallel and perpendicular, respectively. Figure 21 shows that two types of fabrication yielded almost the same x-ray diffraction patterns. The orientation angles and Herman's orientation function were calculated, and are given in Table 8. This observation indicates that liquid crystal molecules orient parallel to the carbon fiber axis, regardless of the initial orientation or fabrication approaches used in this study. The carbon fiber surface has apparently induced molecular orientation of the liquid crystal polymer parallel to the carbon fiber axis. Surface induced orientation is also supported by the fact that the degree of orientation for both the polymer molecules and carbon basal planes is very similar. It also suggests that the most stable state for liquid crystal domains is to align themselves parallel to the carbon fiber surface. This observation is in agreement with previous publications concerning the induced alignment of low molecular weight liquid crystals on smooth carbon surfaces.[34-36]

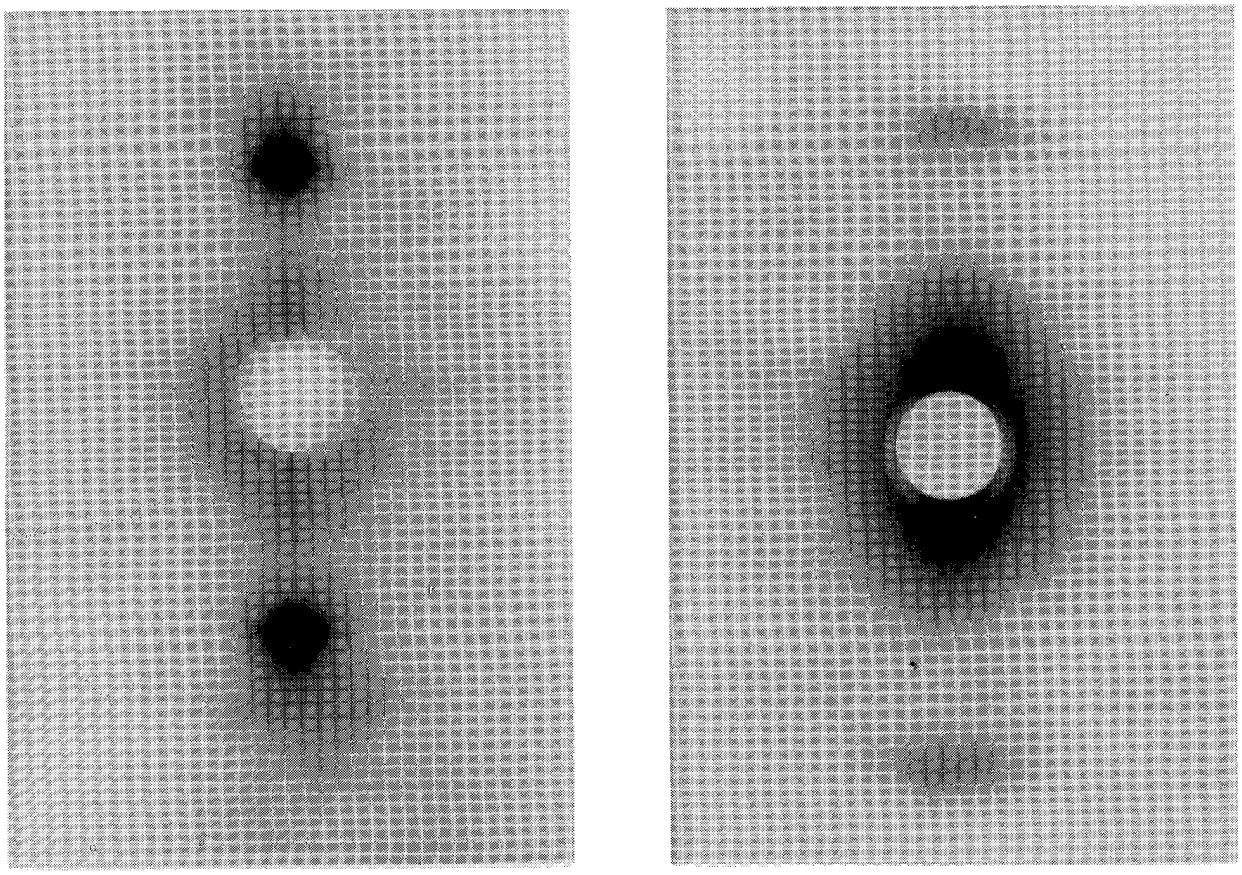

(A) CF

(B) LCP Film

FIGURE 20. X-RAY DIFFRACTION PATTERNS OF NEAT LCP FILM AND CARBON FIBER

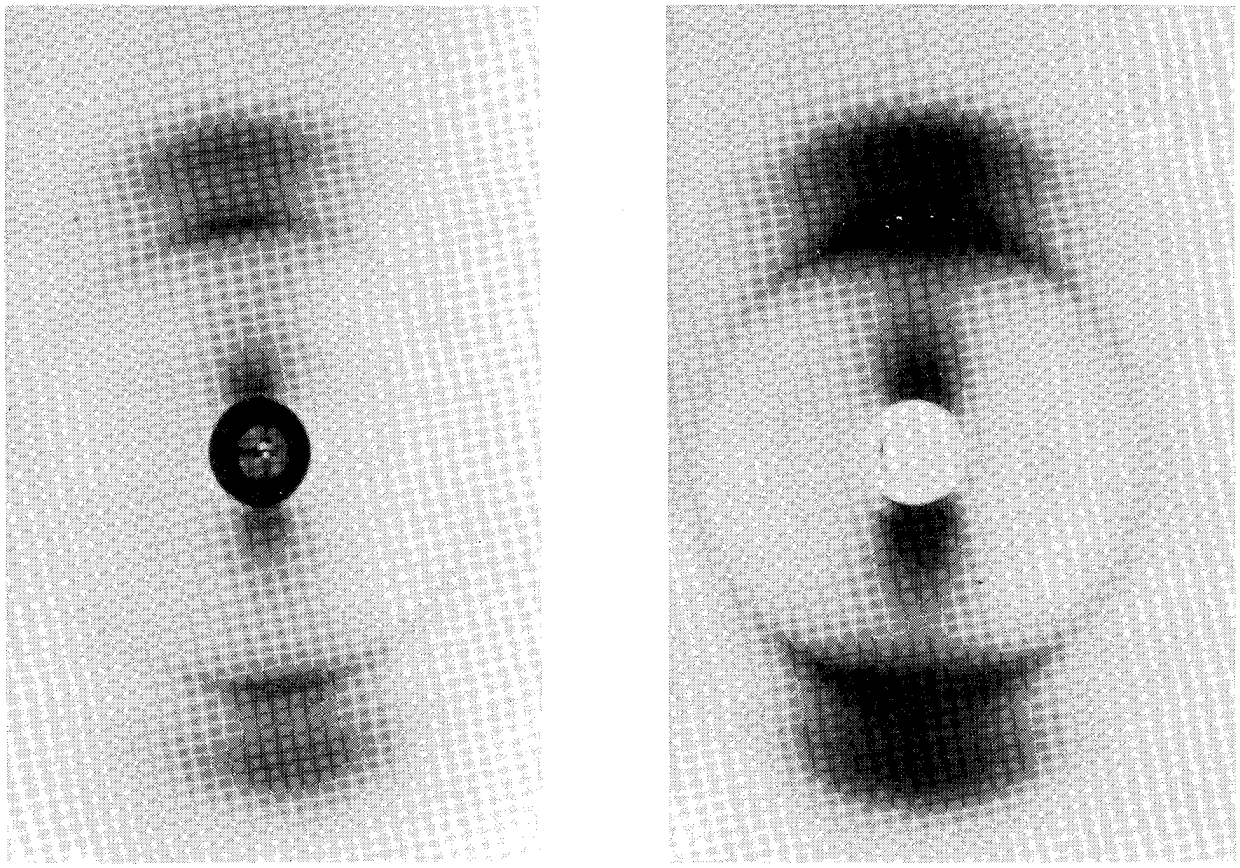

(A) LCP Film Parallel to CF Axis

(B) LCP Film Perpendicular to CF Axis

FIGURE 21. X-RAY DIFFRACTION PATTERNS OF COMPOSITES

TABLE 8. ORIENTATION ANGLES AND HERMAN'S ORIENTATION FUNCTION OF CARBON FIBER AND LCP IN COMPOSITES AND IN NEAT LCP FILM

| Process | Weight % Carbon Fiber | Orientation (Degrees) (1) | | | | Herman's Function (2) | | | |
|---|---|---|---|---|---|---|---|---|---|
| | | <002> CF | | <110> LCP | | <002> CF | | <110> LCP | |
| | | Y (3) | Z | Y | Z | Y | Z | Y | Z |
| LCP Film Parallel to CF Axis | 42 | 21.02 | 24.35 | 23.33 | 23.88 | 0.82 | 0.78 | 0.77 | 0.76 |
| LCP Film Perpendicular to CF Axis | 38 | 23.66 | 23.56 | 23.37 | 25.14 | 0.80 | 0.80 | 0.80 | 0.80 |
| Neat LCP Film | 0 | | | 8.01 | 8.35 | | | 0.96 | 0.97 |

(1) Given as the full width at one-half integral intensity of the <002> carbon fiber or <110> LCP equatorial reflection in degrees. The incident beam direction is indicated as Y or Z (see text). Patterns with the incident beam directed along the X axis are unoriented.

(2) The value of the Herman's orientation function computed from the azimuthal intensity distribution.

(3) X, Y, Z defined as follows:

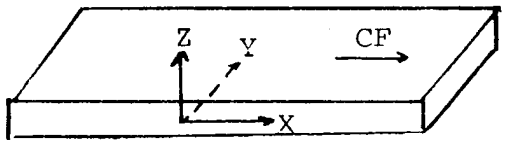

## SECTION 7. CONCLUSIONS AND RECOMMENDATIONS

### 7.1 Conclusions

The following conclusions can be drawn from this study.

(1) LCP/CF prepregs with good fiber distribution uniformity, wet-out, and low void content have been developed using a pultrusion process.

(2) A significant number of mechanical properties of LCP/CF composites are comparable to those of epoxy/CF composites. In particular, LCP/CF composites have superior impact resistance to thermosetting matrix counterparts. However, deficiencies in shear strength and compression strength are apparent. These deficiencies may be attributable to the poor interface adhesion between matrix and fiber.

(3) LCP/CF composites have good property retention until 200°F (67%). Above 200°F, mechanical properties decrease significantly. This may be due to the β-transition of LCP as well as the poor interfacial adhesion between fiber and matrix. This deficiency may be moderated by using LCP compositions with higher β-transitions.

(4) The critical stress intensity factor $K_{1c}$ of LCP is good. However, the key fracture toughness parameter $G_{1c}$ is proportional to $K_{1c}$ and varies inversely with the modulus. This implies that LCP, with a high Young's modulus, may have inadequate toughness to resist extension of an existing crack. This deficiency may also contribute to the poor shear and compression strengths measured on the LCP/CF composites.

## 7.2 Recommendations

(1) Study the effect of carbon fiber surface finish on composite shear strength and compression strength.

(2) Study the effect of high strain carbon fiber on composites properties.

(3) The melt impregnation process may be utilized for the evaluation of composites with other thermoplastic polymer matrices.

SECTION 8. REFERENCES


1. J. T. Hoggatt, "Investigation of Reinforced Thermoplastics for Naval Aircraft Structural Applications," contract N00019-72-C-0526 (1973). Report No. D180-17531-1.

2. G. Husman and J. Hartness, 24th Nat'l. SAMPE Symposium, 24, Book 2, 21 (1979).

3. J. Hartness, 25th Nat'l. SAMPE Symposium, 25, 376 (1980).

4. J. Hartness, 14th Nat'l. SAMPE Technical Conf., 14, 26 (1982).

5. J. Hartness, SAMPE Quarterly, 33, (1983).

6. P. E. McMahon and M. Maximovich, 3rd Internat'l. Conf. on Composite Mtls., Paris (1980).

7. C. H. Sheppard and E. E. House, "Development of Improved Graphite Reinforced Thermoplastic Composites," contract N00019-80-C-0365 (1981). Report No. D180-25870-1.

8. R. B. Rigby, 27th National SAMPE Symposium, 27, 747 (1982).

9. G. R. Belbin, I. Brewster, F. N. Cogswell,1 D. J. Hezzell and M. S. Swerdlow, 2nd Intercontinental SAMPE Conf., Stresa, Italy (1982).

10. J. Hartness and R. Y. Kim, 28th Nat'l SAMPE Symposium, 28, 535 (1983).

11. E. Baer, J. A. Koutsky and A. G. Walton, Polymer Letters, 5, 177 (1967), ibid, 5, 185 (1967).

12. E. W. Fisher and J. Willems, Die Makromoleculare Chemie, 99, 85 (1966).

13. H. Seifert, J. Phys. Chem., Solids, Supplements No. 1, 534 (1967).

14. J. B. Lando and P. D. Frayer, J. Colloid and Interface Sci., 31, 145 (1969).

15. F. Tuinstra and E. Baer, J. Polym. Sci., B8, 861 (1970).

16. J. L. Kardos and F. S. Cheng, and T. L. Tolbert, Polym. Eng. Sci., 13, 455 (1973).

17. S. Y. Hobb, Nature Physical Sci., 234, p. 12 (1971), and 239, 28 (1972).

18. S. Y. Hobb, U.S. Pat. 3,812,077, (1974).

19. F. N. Cogswell, 28th Nat'l. SAMPE Symposium, 28, 528 (1983).

20. H. F. Kuhfuss, and W. J., Jackson, Jr., U.S. Pat. 3778410 (Dec. 11, 1973).

21. Idem, U.S. Pat. 3804805 (Apr. 16, 1974).

22. J. R. Jackson, Jr., and H. F. Kuhfuss, J. Polym. Sci. Polym. Chem. Ed., 14, 2043, (1976).

23. T. C. Pletcher, U.S. Pat. 3991013 and 3991014 (Nov. 9, 1976).

24. J. R. Schaefgen, U.S. Pat. 4075262 (Feb. 21, 1978).

25. J. R. Schaefgen, U.S. Pat. 4118372 (Oct. 3, 1978).

26. R. S. Irwin, U.S. Pat. 4176223 (Nov. 27, 1979).

27. W. J. Jackson, Fr., and H. F. Kuhfuss, U.S. Pat. 4140846 (Feb. 20, 1979).

28. W. J. Jackson, Jr., and J. C. Morris, U.S. Pat. 4181792 (Jan. 1, 1980).

29. G. W. Calundann, U.S. Pat. 4130545 (Dec. 19, 1978).

30. G. W. Calundan, U.S. Pat. 4161470 (Jul. 17, 1979) and U.S Pat. 4184996 (Jan. 22, 1980).

31. S. Baxter and A. B. D. Cassie, J. of Text. Inst., T67 (1945).

32. A. J. East, L. F. Charbonneau and G. W. Calundann, U.S. Pat. 4,330,457, (1982).

33. S. Mostovoy and E. J. Ripling, J. Appl. Poly. Sci., 10, 1351 (1966).

34. L. T. Creagh and A. R. Kmetz, "Cryst. Liq. Cryst.," 24, 59 (1973).

35. A. Derzhanski, L. Komitov and M. Mikarlov, "Krist. und Techn.," 14, 213 (1979).

36. J. Cognard, "Alignment of Nematic Liquid Crystals and their Mixtures," Mol. Cryst. Liq. Cryst. Supplement, Series 1 (1982).

## ACKNOWLEDGEMENTS

The author would like to thank Mr. W. D. Timmons, and Drs. S. K. Garg, G. E. Williams, Y. Ide, P. E. McMahon, M. Jaffe, Z. Gurion and K. Wissbrun for the helpful suggestions and Mr. D. Palangio and Mrs. J. L. Scott for their excellent technical assistance. The author also wishes to acknowledge Mrs. J. E. Hileman for her assistance in the preparation of this report.

| 1. Report No. | 2. Government Accession No. | 3. Recipient's Catalog No. |
|---|---|---|
| NASA CR-172323 | | |

| 4. Title and Subtitle | 5. Report Date |
|---|---|
| LIQUID CRYSTAL POLYESTER-CARBON FIBER COMPOSITES | May 1984 |
| | 6. Performing Organization Code 19240 |
| 7. Author(s) | 8. Performing Organization Report No. |
| Tai-Shung Chung | |
| | 10. Work Unit No. |
| 9. Performing Organization Name and Address | |
| Celanese Research Company<br>86 Morris Avenue<br>Summit, NJ 07901 | 11. Contract or Grant No. NAS1-15749 |
| | 13. Type of Report and Period Covered Contractor Report |
| 12. Sponsoring Agency Name and Address | |
| National Aeronautics and Space Administration<br>Washington, DC 20546 | 14. Sponsoring Agency Code |

15. Supplementary Notes The use of trademarks or names of manufacturers in this report does not constitute endorsement, either expressed or implied, by the National Aeronautics and Space Administration.
Langley Technical Monitor: Vernon L. Bell Final Report - Task 5

16. Abstract Liquid crystal polymers (LCP) have been developed as a thermoplastic matrix for high performance composites. A successful melt impregnation method has been developed which results in the production of continuous carbon fiber (CF) reinforced LCP prepreg tape. Subsequent layup and molding of prepreg into laminates has yielded composites of good quality.

Tensile and flexural properties of LCP/CF composites are comparable to those of epoxy/CF composites. LCP/CF composites have better impact resistance than the latter, although epoxy/CF composites possess superior compression and shear strength. LCP/CF composites have good property retention until 200°F (67% of room temperature value). Above 200°F, mechanical properties are found to decrease significantly.

Experimental results indicate that the poor compression and shear strength may be due to the poor interfacial adhesion between the matrix and carbon fiber as well as inadequate toughness of the LCP matrix. Low mechanical property retention at high temperatures may be attributed to the low β-transition temperature (around 80°C) of the LCP matrix material.

| 17. Key Words (Suggested by Author(s)) | 18. Distribution Statement |
|---|---|
| Liquid crystal polyesters<br>Carbon fiber composites | Unclassified - Unlimited<br>Subject Category 24 |

| 19. Security Classif. (of this report) | 20. Security Classif. (of this page) | 21. No. of Pages | 22. Price |
|---|---|---|---|
| Unclassified | Unclassified | 45 | |



For sale by the National Technical Information Service, Springfield, Virginia 22161